Detection of Imatinib Based on Electrochemical Sensor Constructed Using Biosynthesized Graphene-Silver Nanocomposite

Zhen Wu[1], Jingjing Liu[2], Minmin Liang[3], Haoyue Zheng[3], Chuansheng Zhu[2] and Yan Wang[2]*

[1] Day Chemotherapy Unit, Qianfoshan Hospital, The First Affiliated Hospital of Shandong First Medical University, Jinan, China, [2] Hematology Department, Qianfoshan Hospital, The First Affiliated Hospital of Shandong First Medical University, Jinan, China, [3] Shandong First Medical University, Jinan, China

The establishment of a monitoring technique for imatinib is necessary in clinical and environmental toxicology. Leaf extracts of *Lycoris longituba* were used as reducing agent for the one-step synthesis of reduced graphene oxide-Ag nanocomposites. This nanocomposite was characterized by TEM, FTIR, XRD, and other instruments. Then, the graphene/Ag nanocomposite was used as a modifier to be cemented on the surface of the glassy carbon electrode. This electrode exhibited excellent electrochemical sensing performance. Under the optimal conditions, the proposed electrode could detect imatinib at 10 nM−0.28 mM with a low limit of detection. This electrochemical sensor also has excellent anti-interference performance and reproducibility.

Keywords: biosynthesis, imatinib, silver nanoparticle, graphene composite, *Lycoris longituba*

INTRODUCTION

Cancer is one of the most important diseases facing humanity today. Cancer is lethal because its cells are uncontrolled and proliferate indefinitely and spread throughout the body. Cytostatic agents are the most commonly used class of anti-cancer drugs (Karthik et al., 2017; Liu et al., 2018; Muti and Muti, 2018; Zahed et al., 2018). Their purpose is to inhibit the growth of cancer cells. However, the widespread use of cytostatic agents has caused some other effects, such as on environmental toxicology. Among them, imatinib is a specific inhibitor. Imatinib is frequently used in the treatment of chronic myeloid leukemia and gastrointestinal stromal tumors (Cahill et al., 2017; Hochhaus et al., 2017). For example, patients with chronic myeloid leukemia can use 400 mg of imatinib per day. Previous reports have demonstrated that the cytogenetic and molecular response to imatinib is associated with low plasma concentrations in patients with chronic myeloid leukemia (Serrano et al., 2019; Buclin et al., 2020). Therefore, monitoring of imatinib is necessary, both in the clinical and environmental toxicology fields.

Currently, the detection methods for imatinib include UV-vis spectroscopy (Grante et al., 2014), HPLC (Roth et al., 2010), and electrophoresis (Li et al., 2012; Ahmed et al., 2019). Although these methods can be used for the rapid detection of imatinib, they all have their own drawbacks. For example, UV-vis spectroscopy requires a large number of samples. HPLC methods are slower and require large instruments. The detection sensitivity of electrophoresis method is not enough. Therefore, it is necessary to develop a technique for the rapid detection of imatinib. Electrochemical sensors are a fast and sensitive detection technology. It enables highly sensitive detection of electrochemically active substances. Previous studies have demonstrated that imatinib can be oxidized at lower potentials, so assembling an imatinib-based electrochemical sensor is an approach worth investigating.

Conventional electrochemical sensors use carbon electrodes for the detection of target molecules (Fu et al., 2019; Mahmoudi-Moghaddam et al., 2019; Zhou et al., 2020). Carbon electrodes have a stable electrochemical window and do not react easily with other substances. However, the electrochemical signal of ordinary carbon electrodes is weak (Karimi-Maleh et al., 2021a), so it is difficult to meet the demand of highly sensitive detection. Modification on the surface of ordinary carbon electrodes is a common method to improve the electrochemical activity of sensors (Cao et al., 2019; Alam et al., 2020; Fu et al., 2020). Recent studies have shown that modification of carbon nanomaterials on the surface of glassy carbon electrodes can improve the performance (Karimi-Maleh et al., 2020). For example, modification of graphene on the surface of glassy carbon electrodes can increase the electrical conductivity. However, the layer-layer interaction of graphene is so strong that direct modification can cause agglomeration, which in turn reduces the performance of the sensor (Kumar et al., 2019; Jadoon et al., 2020). Surface modification of polymers allows the surface of graphene to be loaded with tubular energy groups. Under the principle of homogeneous charge repulsion, the layer-layers of graphene can be separated from each other. However, the modified graphene also cannot perform very well due to the poor electrical conductivity of the polymer (Liu et al., 2019). Another strategy is to grow nanoparticles between graphene. The graphene lamellae are separated by nanoparticles. This approach is most beneficial for the modification of electrochemical sensors (Karimi-Maleh et al., 2021b). The presence of nanoparticles can increase the electrochemically active surface area. Also, some nanoparticles have electrochemical catalytic properties that can improve the sensitivity of detection.

Graphene-nanoparticle composites are synthesized by many methods. In recent years, the one-step synthesis of graphene-nanoparticle composites using plant extracts has attracted much attention (Nandgaonkar et al., 2014; Keerthi et al., 2018; Khanam and Hasan, 2019). This method does not require polluting reducing agents and easily controls the size of nanoparticles. For example, Song and Shi (2019) reported the synthesis of graphene/Ag nanocomposites using *Shewanella oneidensis*. Weng et al. (2018) reported the synthesis of graphene/Fe nanocomposites using eucalyptus leaves.

In this work, we chose the leaf extract of *Lycoris longituba* as a reducing agent. The graphene/Ag nanocomposites were reduced by a one-step hydrothermal method. We characterized the conforming materials. The synthesized composites were used for surface modification of glassy carbon electrodes and successfully used for electrochemical detection of imatinib. This novel electrochemical sensor allows highly sensitive detection of imatinib.

EXPERIMENTS

All reagents, including KH_2PO_4, Na_2HPO_4 and silver nitrate were purchased from Macklin Co. Ltd. and used without purification. Graphene oxide (GO) was purchased from Nanin Youshan Biotech Co. Ltd. *Lycoris longituba* was purchased from local nursery. The working electrode, counter electrode and reference electrode were glassy carbon electrode (GCE), Pt wire and Ag/AgCl (3M), respectively. Phosphate buffer solution (PBS) was prepared by mixing stock solutions of 0.1 M disodium hydrogen phosphate and sodium dihydrogen phosphate. The electrochemical determination of imatinib was carried out using a CHI760 electrochemical workstation. Differential pulse voltammetry (DPV) was used for electrochemical recording. The scan range was 0–1.2 V. The pulse amplitude was 50 mV. The pulse width was 0.05 s. The pulse period was 0.5 s.

The XRD pattern of sample was collected by a XRD with Cu Kα (λ = 0.1546 nm) radiation (D8-Advanced, Bruker). Transmission electron microscopy (TEM) image was observed with a JEOL JEM-2100 high-resolution transmission electron microscope. FTIR spectra were collected by a Fourier transform infrared spectroscopy (Nicolet iS5, Thermo Scientific).

To prepare the aqueous extract of *Lycoris longituba*, its crushed leaf (1:20 ratio) was shaken overnight at 200 rpm with water as solvent. Then, the mixture was filtered, and the resulting extract was used for further experiment. Then, 5 mL of the extract
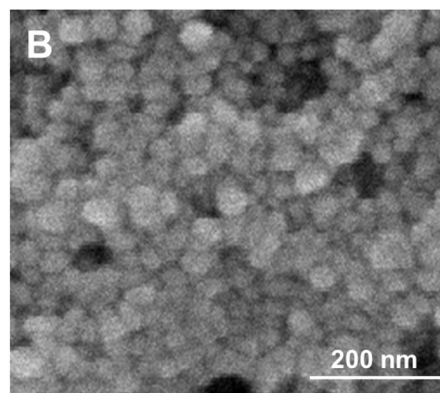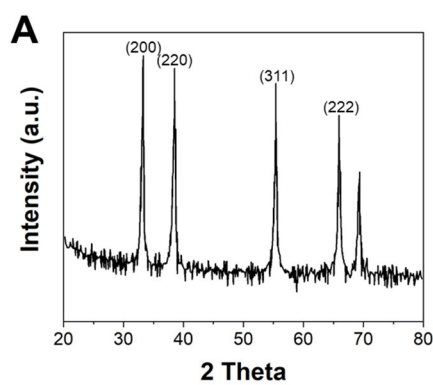

FIGURE 1 | (A) XRD pattern and **(B)** TEM image of biosynthesized G/Ag.

was diluted to 20 mL, and silver nitrate (10 mM) was added to it. This solution was transferred to an autoclave and heated at 120°C for 10 h. The composite was collected after filtration and re-dispersed into water to form a 0.5 mg/mL dispersion (denoted as G/Ag).

RESULTS AND DISCUSSION

Figure 1A shows the XRD pattern of the synthesized G/Ag. It can be seen that four distinct planes of the sample corresponding to (200), (220), (311), and (222) lattice plane of silver face-centered-cube (fcc) crystal (Waterhouse et al., 2001). This result was mated to the reference data in JCPDS file no. 04-0783, suggesting the successful formation of the Ag nanoparticles. Moreover, an additional peak appearing at 26.10° can be also noticed, due to the partial reduced GO sheets to form an ordered crystalline structure (Wang et al., 2013). **Figure 1B** shows the TEM image of the synthesized G/Ag. By the contrast with the background, we can see the layered graphene. On the graphene lamellae we

can see the growing Ag nanoparticles. According to the statistics, the average size of Ag nanoparticles is 24 nm.

Figure 2 shows the FTIR spectra of *Lycoris longituba*, and biosynthesized G/Ag. It can be seen that the extract of *Lycoris longituba* exhibited a series bands at range from 700 to 2,000 cm^{-1}. The absorbance peak at 1,322 cm^{-1} is corresponding to the C–O stretching (Ranjana and Mendhulkar, 2015). In addition, the peak located at 883 cm^{-1} can be assigned to the C–N vibrations of the nitroso groups. These two peaks were also found in the biosynthesized G/Ag, suggesting the biomolecules of the *Lycoris longituba* were attached on the composite surface. The intensity of the oxygen containing groups on the G/Ag is relatively low, indicating the reduction of GO during the hydrothermal treatment.
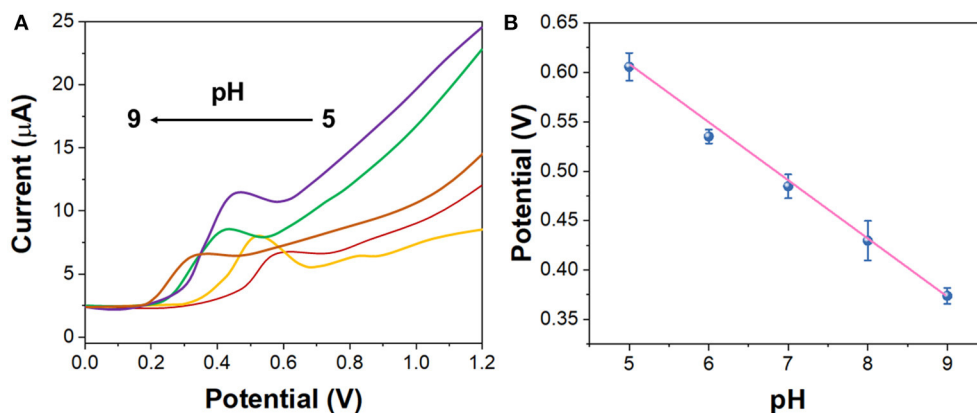
Figure 3A shows the DPV curves of G/Ag/GCE in 10 μM imatinib solution in the pH range between 4.0 and 8.0. It can be seen that the oxidation potential of imatinib shifted to positive direction along with the increase of the pH. **Figure 3B** shows the plot of oxidation potential of imatinib vs. pH value. It can be seen that a slope of 56.9 mV/pH was obtained, suggesting the equal
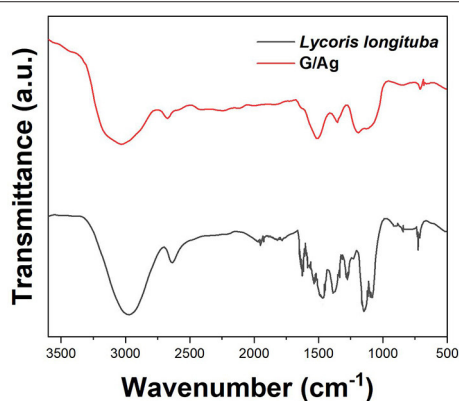
FIGURE 2 | FTIR spectrum of *Lycoris longituba* leaf extract and G/Ag.
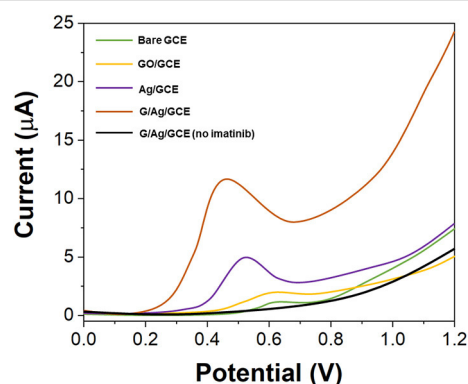
FIGURE 4 | DPV curves of the bare GCE, GO/GCE, Ag/GCE, and G/Ag/GCE toward 10 μM imatinib.

FIGURE 3 | (A) DPV curves of the G/Ag/GCE in 10 μM imatinib solution in the pH range between 4.0 and 8.0. **(B)** Plots of oxidation potential of imatinib vs. pH value.

number of electron and proton were participated in the reaction. In addition, the maximum oxidation response for imatinib was observed at pH = 7.0. Therefore, pH = 7.0 was selected as the optimal condition.

Figure 4 shows the DPV curves of $10\,\mu M$ imatinib using bare GCE, GO/GCE, Ag/GCE, and G/Ag/GCE. It can be seen that the GCE only exhibited a very small oxidation peak with a current response of $1.34\,\mu A$. The modification of GO on the
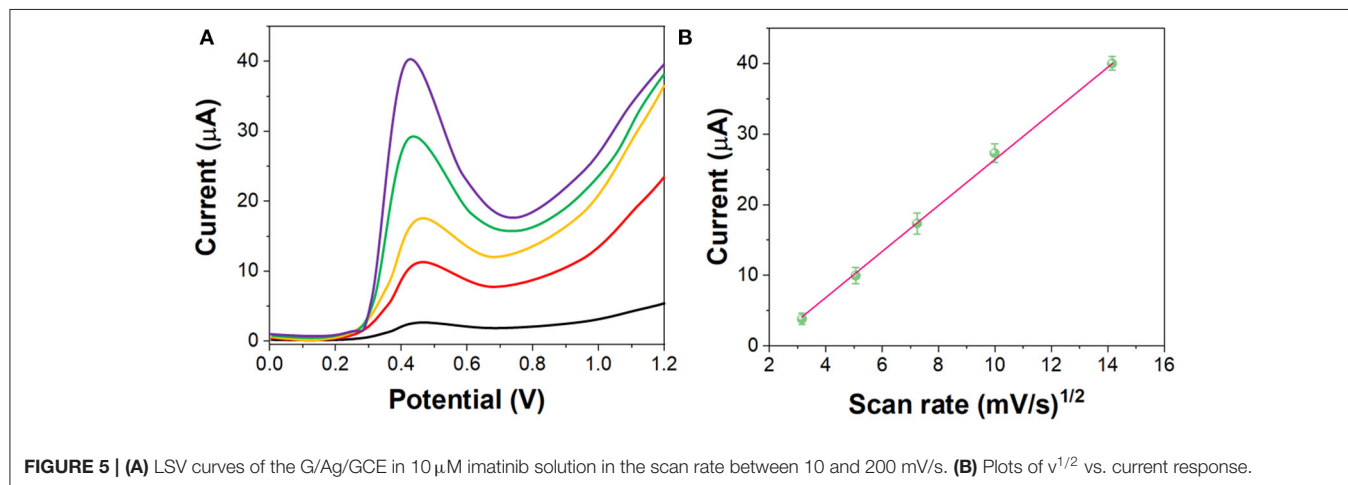

FIGURE 5 | (A) LSV curves of the G/Ag/GCE in $10\,\mu M$ imatinib solution in the scan rate between 10 and 200 mV/s. **(B)** Plots of $v^{1/2}$ vs. current response.
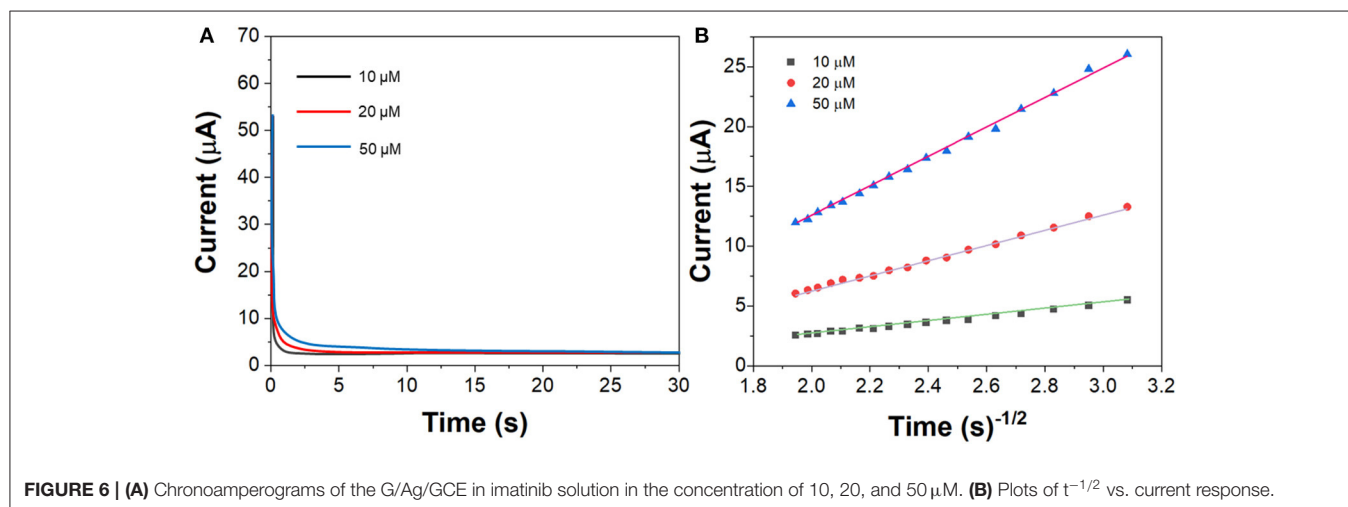

FIGURE 6 | (A) Chronoamperograms of the G/Ag/GCE in imatinib solution in the concentration of 10, 20, and $50\,\mu M$. **(B)** Plots of $t^{-1/2}$ vs. current response.
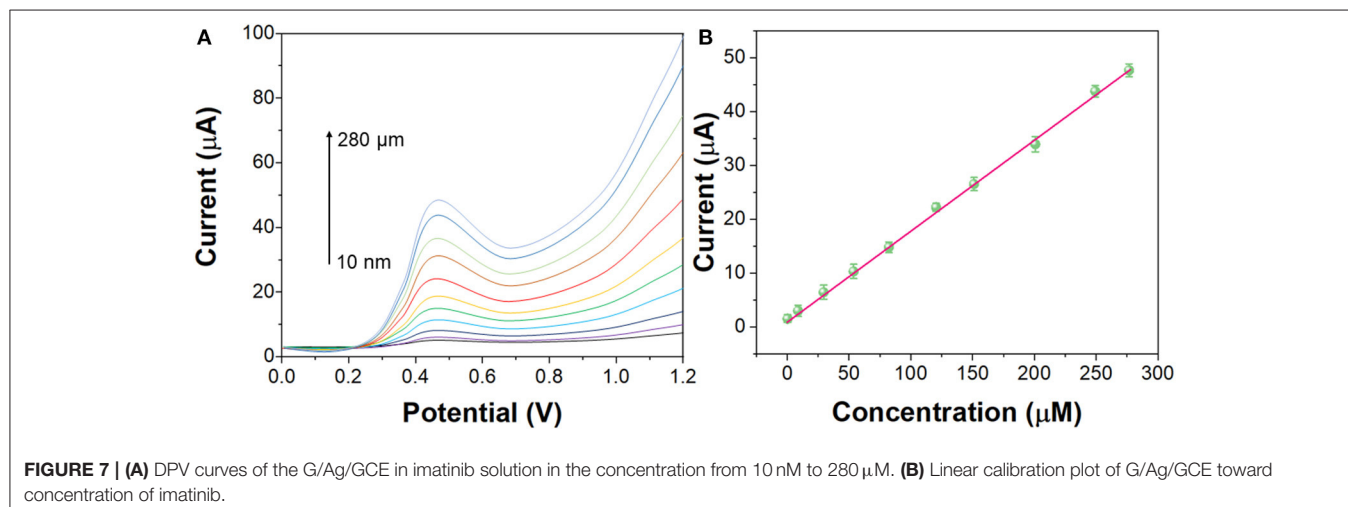

FIGURE 7 | (A) DPV curves of the G/Ag/GCE in imatinib solution in the concentration from 10 nM to $280\,\mu M$. **(B)** Linear calibration plot of G/Ag/GCE toward concentration of imatinib.

GCE showed no clear enhancement. In contrast, the modification of Ag nanopartciles on the GCE surface showed an excellent performance toward imatinib oxidation. An enhanced oxidation peak was observed with 4.52 μA response, suggesting the good electrical conductivity of Ag nanoparticles can enhance the sensing performance. In addition, the G/Ag/GCE showed an even higher response toward imatinib with a much lower oxidation potential, suggesting the combination of Ag and reduced GO can trigger the electrocatalytic reaction with imatinib. The electrocatalytic activity of the Ag nanoaprtciles was observed when the corporation with carbon based materials (Asadian et al., 2017; Liu et al., 2017; Majidi and Ghaderi, 2017; Kumar and Goyal, 2018).

Figure 5 shows the LSV curves of G/Ag/GCE toward 10 μM imatinib with different scan rate (from 10 to 200 mV/s). It can be seen that, the electrochemical oxidation current of the imatinib had a liner relationship with the $v^{1/2}$ while the oxidation potential shifted positively along with the increase of the scan rate, indicating the electrochemical behavior of the imatinib obeyed the diffusion-controlled process (Ivanishchev et al., 2016).

Figure 6A shows the chronoamperograms of G/Ag/GCE toward imatinib with 10, 20, and 50 μM. **Figure 6B** shows the corresponded cottrell plots. The diffusion coefficient was calculated to be ~1.94×10^{-5} cm²/s.
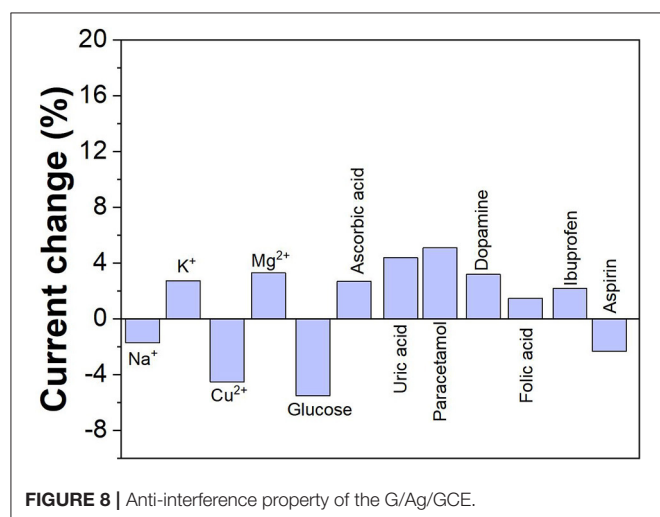
As shown in **Figure 7**, under the optimal experimental conditions, the DPV curves of G/Ag/GCE for different concentrations of imatinib were recorded. G/Ag/GCE has a linear relationship with the concentration of imatinib, with a linear range of 10 nM−280 μM and a detection limit of 1.1 nM (S/N = 3). As shown in **Table 1**, compared with other methods, this method has a lower detection limit and a wider linear range. Although there are some detection methods that work better than our proposed sensors, such as LC/MS/MS and LC/TMS, these methods require large instruments and cannot achieve rapid detection.

In order to discuss the selectivity of G/Ag/GCE, 13 common ions that may interfere with the actual detection of imatinib were investigated in this experiment, as shown in **Figure 8**. The results show that when the concentration of sodium ion, potassium ion, copper ion, manganese ion, cobalt ion, magnesium ion, mercury ion, zinc ion, lead ion, nickel ion, barium ion, aluminum ion and chromium ion is 10 times higher than that of imatinib, there is no obvious interference to the actual detection of imatinib. Therefore, the proposed sensor exhibited an excellent anti-interference property.

The proposed sensor has been then used for determining the content of imatinib in serum samples. Standard addition of imatinib was used. **Table 2** shows the performance of the sensor for real sample analysis. It can be seen that excellent recovery performance was observed for each test, indicating the proposed sensor can be applied for real sample sensing.

TABLE 1 | Electrochemical imatinib sensor performance comparison.

Method	Linear detection range	Detection limit	Reference
SWV	19 nM−1.9 μM	5.55 nM	Chen et al., 2014
MS	0.1 nM−1 μM	–	Friedecký et al., 2015
DPV	10 nM−200 μM	7.39 nM	Hatamluyi and Es'haghi, 2017
DPV	30 nM−0.25 μM	6.3 nM	Brycht et al., 2016
LC/MS/MS	100 nM−7.091 μM	0.1 μM	Andriamanana et al., 2013
Liquid chromatography-tandem mass spectrometry	20 nM−2.052 μM	–	Yang et al., 2013
DPV	10 nM-280 μM	1.1 nM	This work

CONCLUSIONS

The stable Ag nanoparticles were synthesized with the reduction of GO using leaf extracts of *Lycoris longituba* under hydrothermal condition. TEM, XRD and FTIR were used for characterizations. Based on the enhancement effect of imatinib

TABLE 2 | Electrochemical determination of imatinib content in serum samples using G/Ag/GCE.

Sample	Detected (nM)	Added (nM)	Detected (nM)	Recovery (%)
1	0	10.00	9.77	97.70
2	0	20.00	20.47	102.35
3	0	50.00	50.44	100.88
4	0	100.00	99.36	99.36

FIGURE 8 | Anti-interference property of the G/Ag/GCE.

on the electrochemical oxidation signal, an electrochemical sensor was constructed using G/Ag nanocomposite. Under the optimal experimental conditions, a linear range of imatinib detection was obtained between 10 nM and 280 μM with a limit of detection of 1.1 nM. The proposed G/Ag/GCE showed an excellent anti-interference property. In addition, it can be applied to the detection of imatinib in real serum sample.

DATA AVAILABILITY STATEMENT

The original contributions presented in the study are included in the article/supplementary material, further inquiries can be directed to the corresponding author/s.

AUTHOR CONTRIBUTIONS

ZW, YW, and JL conceived of the study. YW and ZW supervised the development program, collected materials characterization. ML, CZ, and HZ received and curated samples and analytical records. HZ, ZW, and YW wrote the manuscript. All authors read and approved of the manuscript.

FUNDING

REFERENCES

Ahmed, O. S., Malý, M., Ladner, Y., Philibert, L., Dubský, P., and Perrin, C. (2019). Influence of salt and acetonitrile on the capillary zone electrophoresis analysis of imatinib in plasma samples. *Electrophoresis* 40, 2810–2819. doi: 10.1002/elps.201900188

Alam, A. U., Clyne, D., Jin, H., Hu, N.-X., and Deen, M. J. (2020). Fully integrated, simple, and low-cost electrochemical sensor array for in situ water quality monitoring. *ACS Sens.* 5, 412–422. doi: 10.1021/acssensors.9b02095

Andriamanana, I., Gana, I., Duretz, B., and Hulin, A. (2013). Simultaneous analysis of anticancer agents bortezomib, imatinib, nilotinib, dasatinib, erlotinib, lapatinib, sorafenib, sunitinib and vandetanib in human plasma using LC/MS/MS. *J. Chromatogr. B* 926, 83–91. doi: 10.1016/j.jchromb.2013.01.037

Asadian, E., Shahrokhian, S., Zad, A. I., and Ghorbani-Bidkorbeh, F. (2017). Glassy carbon electrode modified with 3D graphene–carbon nanotube network for sensitive electrochemical determination of methotrexate. *Sens. Actuators B Chem.* 239, 617–627. doi: 10.1016/j.snb.2016.08.064

Brycht, M., Kaczmarska, K., Uslu, B., Ozkan, S. A., and Skrzypek, S. (2016). Sensitive determination of anticancer drug imatinib in spiked human urine samples by differential pulse voltammetry on anodically pretreated boron-doped diamond electrode. *Diam. Relat. Mater.* 68, 13–22. doi: 10.1016/j.diamond.2016.05.007

Buclin, T., Thoma, Y., Widmer, N., André, P., Guidi, M., Csajka, C., et al. (2020). The steps to therapeutic drug monitoring: a structured approach illustrated with imatinib. *Front. Pharmacol.* 11:177. doi: 10.3389/fphar.2020.00177

Cahill, K. N., Katz, H. R., Cui, J., Lai, J., Kazani, S., Crosby-Thompson, A., et al. (2017). KIT inhibition by imatinib in patients with severe refractory asthma. *N. Engl. J. Med.* 376, 1911–1920. doi: 10.1056/NEJMoa1613125

Cao, Y., Wang, L., Shen, C., Wang, C., Hu, X., and Wang, G. (2019). An electrochemical sensor on the hierarchically porous Cu-BTC MOF platform for glyphosate determination. *Sens. Actuators B Chem.* 283, 487–494. doi: 10.1016/j.snb.2018.12.064

Chen, H., Wang, X., Chopra, S., Adams, E., and Van Schepdael, A. (2014). Development and validation of an indirect pulsed electrochemical detection method for monitoring the inhibition of Abl1 tyrosine kinase. *J. Pharm. Biomed. Anal.* 90, 52–57. doi: 10.1016/j.jpba.2013.11.022

Friedecký, D., Mičová, K., Faber, E., Hrdá, M., Široká, J., and Adam, T. (2015). Detailed study of imatinib metabolization using high-resolution mass spectrometry. *J. Chromatogr. A* 1409, 173–181. doi: 10.1016/j.chroma.2015.07.033

Fu, L., Zheng, Y., Zhang, P., Zhang, H., Wu, M., Zhang, H., et al. (2019). An electrochemical method for plant species determination and classification based on fingerprinting petal tissue. *Bioelectrochemistry* 129, 199–205. doi: 10.1016/j.bioelechem.2019.06.001

Fu, L., Zheng, Y., Zhang, P., Zhang, H., Xu, Y., Zhou, J., et al. (2020). Development of an electrochemical biosensor for phylogenetic analysis of Amaryllidaceae

based on the enhanced electrochemical fingerprint recorded from plant tissue. *Biosens. Bioelectron.* 159:112212. doi: 10.1016/j.bios.2020.112212

Grante, I., Actins, A., and Orola, L. (2014). Protonation effects on the UV/Vis absorption spectra of imatinib: a theoretical and experimental study. *Spectrochim. Acta. Mol. Biomol. Spectrosc.* 129, 326–332. doi: 10.1016/j.saa.2014.03.059

Hatamluyi, B., and Es'haghi, Z. (2017). A layer-by-layer sensing architecture based on dendrimer and ionic liquid supported reduced graphene oxide for simultaneous hollow-fiber solid phase microextraction and electrochemical determination of anti-cancer drug imatinib in biological samples. *J. Electroanal. Chem.* 801, 439–449. doi: 10.1016/j.jelechem.2017.08.032

Hochhaus, A., Larson, R. A., Guilhot, F., Radich, J. P., Branford, S., Hughes, T. P., et al. (2017). Long-term outcomes of imatinib treatment for chronic myeloid leukemia. *N. Engl. J. Med.* 376, 917–927. doi: 10.1056/NEJMoa1609324

Ivanishchev, A. V., Churikov, A. V., Ivanishcheva, I. A., and Ushakov, A. V. (2016). Lithium diffusion in Li 3 V 2 (PO 4) 3-based electrodes: a joint analysis of electrochemical impedance, cyclic voltammetry, pulse chronoamperometry, and chronopotentiometry data. *Ionics* 22, 483–501. doi: 10.1007/s11581-015-1568-y

Jadoon, T., Mahmood, T., and Ayub, K. (2020). Silver-graphene quantum dots based electrochemical sensor for trinitrotoluene and p-nitrophenol. *J. Mol. Liq.* 306:112878. doi: 10.1016/j.molliq.2020.112878

Karimi-Maleh, H., Alizadeh, M., Orooji, Y., Karimi, F., Baghayeri, M., Rouhi, J., et al. (2021a). Guanine-based DNA biosensor amplified with Pt/SWCNTs nanocomposite as analytical tool for nanomolar determination of daunorubicin as an anticancer drug: a docking/experimental investigation. *Ind. Eng. Chem. Res.* 60, 816–823. doi: 10.1021/acs.iecr.0c04698

Karimi-Maleh, H., Ayati, A., Davoodi, R., Tanhaei, B., Karimi, F., Malekmohammadi, S., et al. (2021b). Recent advances in using of chitosan-based adsorbents for removal of pharmaceutical contaminants: a review. *J. Clean. Prod.* 291:125880. doi: 10.1016/j.jclepro.2021.125880

Karimi-Maleh, H., Orooji, Y., Ayati, A., Qanbari, S., Tanhaei, B., Karimi, F., et al. (2020). Recent advances in removal techniques of Cr(VI) toxic ion from aqueous solution: a comprehensive review. *J. Mol. Liq.* 329:115062. doi: 10.1016/j.molliq.2020.115062

Karthik, R., Sasikumar, R., Chen, S.-M., Vinoth Kumar, J., Elangovan, A., Muthuraj, V., et al. (2017). A highly sensitive and selective electrochemical determination of non-steroidal prostate anti-cancer drug nilutamide based on f-MWCNT in tablet and human blood serum sample. *J. Colloid Interface Sci.* 487, 289–296. doi: 10.1016/j.jcis.2016.10.047

Keerthi, M., Akilarasan, M., Chen, S.-M., Kogularasu, S., Govindasamy, M., Mani, V., et al. (2018). One-pot biosynthesis of reduced graphene oxide/prussian blue microcubes composite and its sensitive detection of prophylactic drug dimetridazole. *J. Electrochem. Soc.* 165:B27. doi: 10.1149/2.0591802jes

Khanam, P. N., and Hasan, A. (2019). Biosynthesis and characterization of graphene by using non-toxic reducing agent from allium cepa extract: anti-bacterial properties. *Int. J. Biol. Macromol.* 126, 151–158. doi: 10.1016/j.ijbiomac.2018.12.213

Kumar, N., and Goyal, R. N. (2018). Silver nanoparticles decorated graphene nanoribbon modified pyrolytic graphite sensor for determination of histamine. *Sens. Actuators Chem.* 268, 383–391. doi: 10.1016/j.snb.2018.04.136

Kumar, S., Bukkitgar, S. D., Singh, S., Singh, V., Reddy, K. R., Shetti, N. P., et al. (2019). Electrochemical sensors and biosensors based on graphene functionalized with metal oxide nanostructures for healthcare applications. *Chem. Select.* 4, 5322–5337. doi: 10.1002/slct.201803871

Li, J., Huang, Y., Huang, L., Ye, L., Zhou, Z., Xiang, G., et al. (2012). Determination of imatinib mesylate and related compounds by field amplified sample stacking with large volume sample injection capillary electrophoresis. *J. Pharm. Biomed. Anal.* 70, 26–31. doi: 10.1016/j.jpba.2012.05.010

Liu, S., Lai, G., Zhang, H., and Yu, A. (2017). Amperometric aptasensing of chloramphenicol at a glassy carbon electrode modified with a nanocomposite consisting of graphene and silver nanoparticles. *Microchim. Acta* 184, 1445–1451. doi: 10.1007/s00604-017-2138-y

Liu, Y., Liang, Y., Yang, R., Li, J., and Qu, L. (2019). A highly sensitive and selective electrochemical sensor based on polydopamine functionalized graphene and molecularly imprinted polymer for the 2, 4-dichlorophenol recognition and detection. *Talanta* 195, 691–698. doi: 10.1016/j.talanta.2018.11.052

Liu, Y., Wei, M., Hu, Y., Zhu, L., and Du, J. (2018). An electrochemical sensor based on a molecularly imprinted polymer for determination of anticancer drug Mitoxantrone. *Sens. Actuators B Chem.* 255, 544–551. doi: 10.1016/j.snb.2017.08.023

Mahmoudi-Moghaddam, H., Tajik, S., and Beitollahi, H. (2019). Highly sensitive electrochemical sensor based on La3+-doped Co3O4 nanocubes for determination of sudan I content in food samples. *Food Chem.* 286, 191–196. doi: 10.1016/j.foodchem.2019.01.143

Majidi, M. R., and Ghaderi, S. (2017). Facile fabrication and characterization of silver nanodendrimers supported by graphene nanosheets: a sensor for sensitive electrochemical determination of Imidacloprid. *J. Electroanal. Chem.* 792, 46–53. doi: 10.1016/j.jelechem.2017.03.028

Muti, M., and Muti, M. (2018). Electrochemical monitoring of the interaction between anticancer drug and DNA in the presence of antioxidant. *Talanta* 178, 1033–1039. doi: 10.1016/j.talanta.2017.08.089

Nandgaonkar, A. G., Wang, Q., Fu, K., Krause, W. E., Wei, Q., Gorga, R., et al. (2014). A one-pot biosynthesis of reduced graphene oxide (RGO)/bacterial cellulose (BC) nanocomposites. *Green Chem.* 16, 3195–3201. doi: 10.1039/C4GC00264D

Ranjana, S., and Mendhulkar, V. D. (2015). FTIR studies and spectrophotometric analysis of natural antioxidants, polyphenols and flavonoids in *Abutilon indicum* (Linn) sweet leaf extract. *J. Chem. Pharm. Res.* 7, 205–211.

Roth, O., Spreux-Varoquaux, O., Bouchet, S., Rousselot, P., Castaigne, S., Rigaudeau, S., et al. (2010). Imatinib assay by HPLC with photodiode-array UV detection in plasma from patients with chronic myeloid leukemia: comparison with LC-MS/MS. *Clin. Chim. Acta* 411, 140–146. doi: 10.1016/j.cca.2009.10.007

Serrano, C., Mariño-Enríquez, A., Tao, D. L., Ketzer, J., Eilers, G., Zhu, M., et al. (2019). Complementary activity of tyrosine kinase inhibitors against secondary kit mutations in imatinib-resistant gastrointestinal stromal tumours. *Br. J. Cancer* 120, 612–620. doi: 10.1038/s41416-019-0389-6

Song, X., and Shi, X. (2019). Biosynthesis of Ag/reduced graphene oxide nanocomposites using Shewanella oneidensis MR-1 and their antibacterial and catalytic applications. *Appl. Surf. Sci.* 491, 682–689. doi: 10.1016/j.apsusc.2019.06.154

Wang, M. Y., Shen, T., Wang, M., Zhang, D., and Chen, J. (2013). One-pot green synthesis of Ag nanoparticles-decorated reduced graphene oxide for efficient nonenzymatic H2O2 biosensor. *Mater. Lett.* 107, 311–314. doi: 10.1016/j.matlet.2013.06.031

Waterhouse, G. I., Bowmaker, G. A., and Metson, J. B. (2001). The thermal decomposition of silver (I, III) oxide: a combined XRD, FT-IR and Raman spectroscopic study. *Phys. Chem. Chem. Phys.* 3, 3838–3845. doi: 10.1039/b103226g

Weng, X., Lin, Z., Xiao, X., Li, C., and Chen, Z. (2018). One-step biosynthesis of hybrid reduced graphene oxide/iron-based nanoparticles by eucalyptus extract and its removal of dye. *J. Clean. Prod.* 203, 22–29. doi: 10.1016/j.jclepro.2018.08.158

Yang, J. S., Cho, E. G., Huh, W., Ko, J.-W., Jung, J. A., and Lee, S.-Y. (2013). Rapid determination of imatinib in human plasma by liquid chromatography-tandem mass spectrometry: application to a pharmacokinetic study. *Bull. Korean Chem. Soc.* 34, 2425–2430. doi: 10.5012/bkcs.2013.34.8.2425

Zahed, F. M., Hatamluyi, B., Lorestani, F., and Es'haghi, Z. (2018). Silver nanoparticles decorated polyaniline nanocomposite based electrochemical sensor for the determination of anticancer drug 5-fluorouracil. *J. Pharm. Biomed. Anal.* 161, 12–19. doi: 10.1016/j.jpba.2018.08.004

Zhou, J., Zheng, Y., Zhang, J., Karimi-Maleh, H., Xu, Y., Zhou, Q., et al. (2020). Characterization of the electrochemical profiles of lycoris seeds for species identification and infrageneric relationships. *Anal. Lett.* 53, 2517–2528. doi: 10.1080/00032719.2020.1746327